A KINETIC ALIGNMENT OF ORTHOLOGOUS IMP DEHYDROGENASES[†]

SUPPLEMENTARY INFORMATION

Thomas V. Riera[¶], Wen Wang[¶] Helen R. Josephine[¶] and Lizbeth Hedstrom[¶§*]

Departments of [¶]Biochemistry and [§]Chemistry, Brandeis University, Waltham, MA 02454 USA

Figure S1. Equilibrium fluorescence in arbitrary fluorescence units (AFU) of *C. parvum* IMPDH versus varying IMP (A) or NAD^+ (B). The fluorescence has been corrected for inner filter effects and nonspecific quenching as described in Materials and Methods. Binding reactions with IMP or NAD^+ were done with 0.12 μM enzyme, 50 mM Tris-Cl, pH 8.0, 100 mM KCl, and 1 mM DTT at 25 °C.

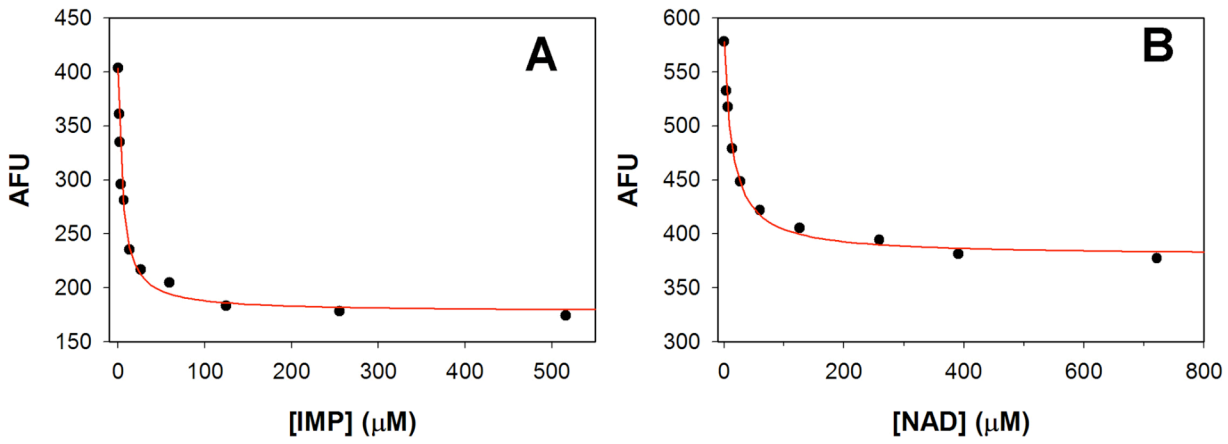

Figure S2. Pre-steady-state reaction of *Cp*IMPDH monitored by absorbance. (A) Progress curve for the reaction of E•IMP with NAD^+ monitored by absorbance. Final concentrations after mixing are: 2.7 μM *Cp*IMPDH, 500 μM IMP, 5 mM NAD^+, 50 mM Tris-Cl, pH 8.0, 100 mM KCl, and 1 mM DTT . The data were fit by eq 6 (red curve). (B) The dependence of the value of k_{obs} versus NAD^+ concentration. These data were fit by eq 8 (red curve).

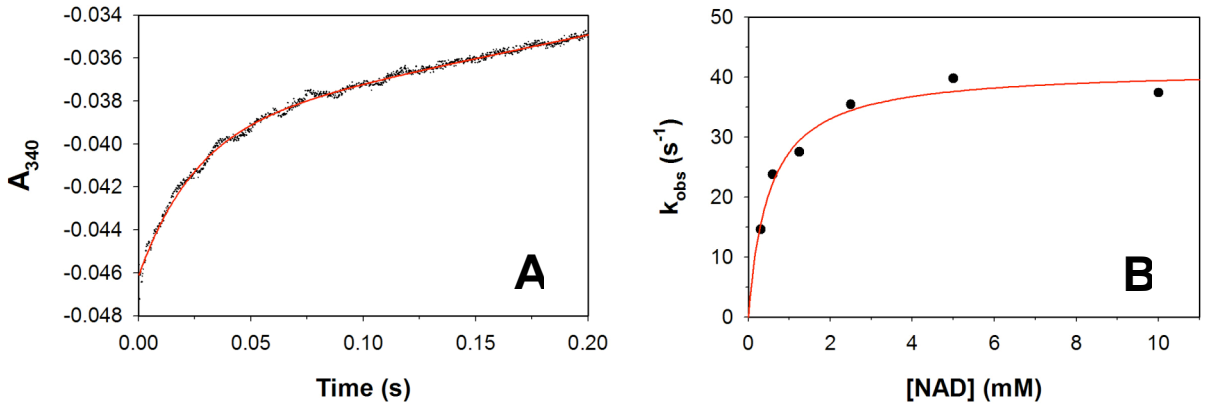

Figure S3. Pre-steady-state reaction of *Cp*IMPDH monitored by fluorescence. (A) Progress curve for the reaction of E•IMP with NAD^+ monitored by fluorescence. Conditions as in Fig. S2A except 1 μM *Cp*IMPDH. (B) The dependence of the value of k_{obs} versus NAD^+ concentration. These data were fit by eq 8 (red curve).

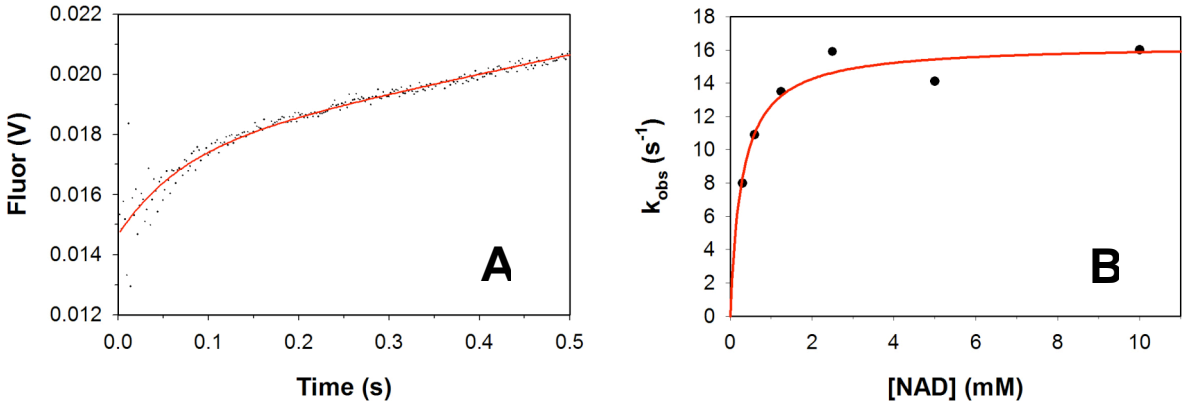

Calculation of k_{HOH} for the CpIMPDH reaction

A solvent isotope effect on k_{cat}, steady-state accumulation of the E-XMP* intermediate, and pre-steady-state bursts of NADH production and release all implicate hydrolysis as rate-limiting in *Cp*IMPDH. The rate of NADH release (k_9) is only 6-fold faster than k_{cat} signifying that it is partially rate-limiting. As in the case of *Tf*IMPDH, NADH release and hydrolysis are irreversible allowing k_{cat} to be simplified to

$$k_{cat} = (k_9 k_{HOH*})/(k_9 + k_{HOH*}) \quad (9)$$

where k_{HOH*} is the observed rate of hydrolysis (*1*). Hydrolysis of E-XMP* requires the closed conformation of the flap, governed by K_c, allowing the intrinsic rate of hydrolysis (k_{HOH}) to be calculated from k_{HOH*} using eq 10.

$$k_{HOH} = k_{HOH*}/(K_c/(1 + K_c)) \quad (10)$$

From eq 9 and 10, $k_{HOH} = 3.9\ s^{-1}$, indistinguishable from the rate for the *T. foetus* enzyme.

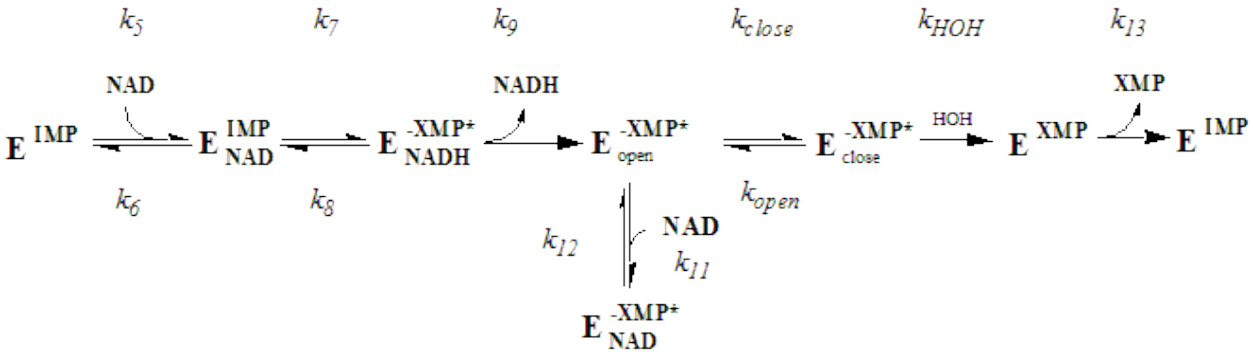

Scheme S1. Kinetic scheme used for global fits of the *Cp*IMPDH reaction.

Global Fit Analysis of the CpIMPDH reaction

The progress curves for the reaction of *Cp*IMPDH monitored by fluorescence and absorbance stopped-flow spectroscopy were globally fit using the program DynaFit (*2*). Signal

response factors for the fluorescence data were calculated by normalizing the linear steady-state regions of the fluorescence and absorbance data. Factors were calculated for each concentration of NAD^+ to adjust for inner filter effects.

The experiment monitored the reaction of the pre-formed E•IMP complex with NAD^+ at saturating IMP concentrations where the association of IMP is fast. Therefore, there are no experimental data to constrain the rate constants for the binding of IMP. The data were fit using the mechanism of Scheme S1. The value of k_{HOH} was fixed to 3.9 s^{-1} as calculated above and k_{13} was set to 200 s^{-1} based on the XMP binding kinetics described in the text. Values of k_{close} and k_{open} were made arbitrarily fast such that the equilibrium constant $K_c = 4$, as determined by multiple inhibitor experiments (*3*). The fits are shown in Figure 3 and the values are listed in Table S1. These data do not contain adequate constraints on the rates of NAD^+ binding to E-XMP*. Therefore, these values are not well-determined and only estimates are provided. However, the value of k_{12}/k_{11} was consistently determined to be 200-400 μM.

Two features arise from the fit results for NAD^+ binding to E•IMP. First, binding is essentially irreversible. The best fit value of k_6 is ~0 s^{-1} and values of k_6 greater than 0.1 s^{-1} result in poor fits to the data. Therefore, $k_6 \leq 0.1$ s^{-1}. Second, the value of k_5 is comparable to k_{cat}/K_M for NAD^+. Together, these observations indicate that NAD^+ is a sticky substrate, whereby the E•IMP•NAD^+ complex reacts before it dissociates. Therefore, the value of $K_d \leq 2.3$ μM for NAD^+ binding to the E•IMP binary complex, which is at least 6x higher than the affinity of NAD^+ for free enzyme.

Based on Scheme S1, expressions for k_{cat} (eq 11) and $K_{M\,NAD^+}$ (eq 12) were derived using the King-Altman method (*4*).

$$k_{cat} = (k_7 k_9 k_{close} k_{HOH} k_{13})/A \qquad (11)$$

$$K_{M\ NAD^+} = [(k_{close}k_{HOH}k_{13})(k_6k_8+k_6k_9+k_7k_9)]/(k_5A) \quad (12)$$

$$A = (k_8k_{close}k_{HOH}k_{13}+ k_9k_{close}k_{HOH}k_{13}+ k_7k_{close}k_{HOH}k_{13}+ k_7k_9k_{open}k_{13}+ k_7k_9k_{HOH}k_{13}+ k_7k_9k_{close}k_{13}+k_7k_9k_{close}k_{HO\mathit{H}}) \quad (13)$$

Using the values from Table S1 for *Cp*IMPDH, $k_{cat} = 1.8\ s^{-1}$ and $K_{M\ NAD^+} = 40\ \mu M$ were calculated from eq 11 and 12 respectively.

Table S1. Values of the rate constants from Scheme S1 and S2 for *Cp*IMPDH and hIMPDH2 respectively.[a]

rate constant	*Cp*IMPDH	hIMPDH2
k_5 ($M^{-1}s^{-1}$)	$(4.4 \pm 0.1) \times 10^4$	1×10^{6} [b]
k_6 (s^{-1})	≤ 0.1 [c]	80 ± 1
k_7 (s^{-1})	44 ± 3	12 ± 0.4
k_8 (s^{-1})	87 ± 6	7.4 ± 0.6
k_9 (s^{-1})	14 ± 1	12 ± 0.3 [d]
k_{11} ($M^{-1}s^{-1}$)	$\sim 4 \times 10^{6}$ [e]	1×10^{6} [f]
k_{12} (s^{-1})	~800 [e]	590 [f]
k_{12}/k_{11} (μM)	200-400[e]	590 [f]
k_{close} (s^{-1})	400 [f]	nd[g]
k_{open} (s^{-1})	100 [f]	nd[g]
k_{conf} (s^{-1})	na[h]	1.0 ± 0.1
k_{HOH} (s^{-1})	3.9 [f]	1 [f]
k_{13} (s^{-1})	200 [f]	nd [g]

[a] Values from the global fits of the absorbance and fluorescence stopped-flow data using the program DynaFit. [b] The slowest value which fits the data. Faster values also work well. [c] Estimated upper limit due to the high commitment to catalysis as described in the text. [d] k_{burst} from the local fit analysis. [e] Approximate values. The individual rates are not well determined; however, the ratio k_{12}/k_{11} was consistently 200-400 μM. [f] Fixed value used for fitting as described in the text. [g] not determined. [h] not applicable.

Figure S4. Pre-steady-state reaction for hIMPDH2. Enzyme and saturating IMP were combined with NAD^+ at time 0 in 50 mM Tris-Cl, pH 8.0, 100 mM KCl, and 1 mM DTT at 25 °C. (A) Final concentrations after mixing are 4 μM enzyme, 2 mM IMP, and 200 μM NAD^+. The fluorescence time course displays two exponential phases followed by a linear steady-state. These data were fit by eq 7 (red curve). (B) Final concentrations after mixing are 3.5 μM enzyme, 2 mM IMP, and 400 μM NAD^+. The absorbance time course displays a single exponential phase followed by a linear steady-state. These data were fit by eq 6 (red curve).

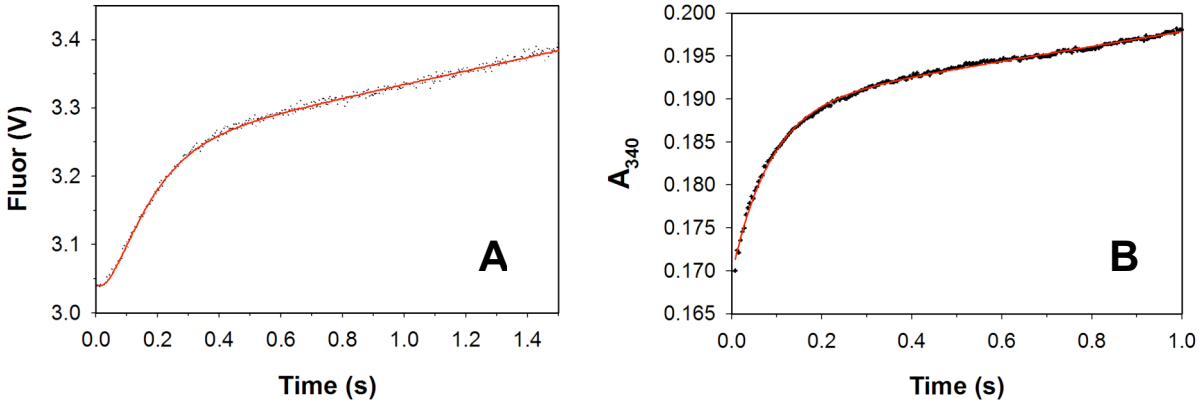

Table S2. The pre-steady state reaction of hIMPDH2 monitored by absorbance.

Enzyme (μM)	NAD^+ μM	k_{obs} (s^{-1})
1.0	400	14 ± 1
1.8	400	13 ± 1
3.5	400	12 ± 1
3.5	1000	15 ± 1

Global Fit Analysis of the hIMPDH2 reaction

The pre-steady-state reaction of E•IMP with NAD^+ for hIMPDH2 was also examined by DynaFit. The mechanism of Scheme S2 was used for fitting. The concentration of IMP used in

these experiments is 2 mM, so IMP binding was modeled as saturated. In the absence of information about the flap equilibrium, we have modeled this step as irreversible for simplicity. Due to its low affinity binding to enzyme, XMP release was modeled as simultaneous with hydrolysis. To account for NAD^+ substrate inhibition, the values of k_{11} and k_{12} were set arbitrarily fast such that $k_{12}/k_{11} = K_{ii}$ = 590 μM (*5*). The global fits supported the assignment of k_{burst} to NADH release, so k_9 was fixed to 12 s^{-1} from the local fit analysis. The value of k_5 was fixed to 1 x 10^6 $M^{-1}s^{-1}$. Slower values resulted in poor fits while faster rates worked equally well. Fixing these values served to further constrain the remaining parameters. The values of the rate constants are listed in Table S2 and the resulting fits are shown in Figure 4.

The value of k_{HOH} was calculated from the values of k_{cat} and the solvent isotope effect as follows. The fractional contribution of k_{HOH} to k_{cat} (*f*) is given by

$$f = ({}^{D2O}k_{cat} - 1)/({}^{D2O}k_{HOH} - 1) \quad (14)$$

where ${}^{D2O}k_{cat}$ is the solvent isotope effect on k_{cat} and ${}^{D2O}k_{HOH}$ is the intrinsic isotope effect on hydrolysis, allowing k_{HOH} to be calculated from eq 15.

$$k_{HOH} = k_{cat}/f \quad (15)$$

Assuming the intrinsic isotope effect is 3, as observed in the reaction of *Cp*IMPDH as well as in the reaction of serine proteases (*6*), then f = 0.4, k_{HOH} = 1 s^{-1} and k = 0.7 s^{-1} for the other rate-limiting step (*7*). From this analysis, the value of k_{HOH} was fixed to 1 s^{-1} for global fitting resulting in a fitted value for k_{close} of 1 s^{-1}. Thus, both the solvent isotope effect and stopped-flow experiments support an additional rate-limiting step.

Consistent with the local fit analysis, the hydride transfer step is similar in rate to NADH release. The calculated value of K_H for this step is 1.6. From these fits, NAD^+ binding to the E•IMP complex has a K_d = 80 μM. Substantial isotope effects have been observed on *V/K*

(NAD^+) indicating that NAD^+ is not a sticky substrate for the hIMPDH2 (*5, 8*). This predicts that the value of $k_6 \geq k_7 = 12\ s^{-1}$. This prediction is fulfilled by the fits.

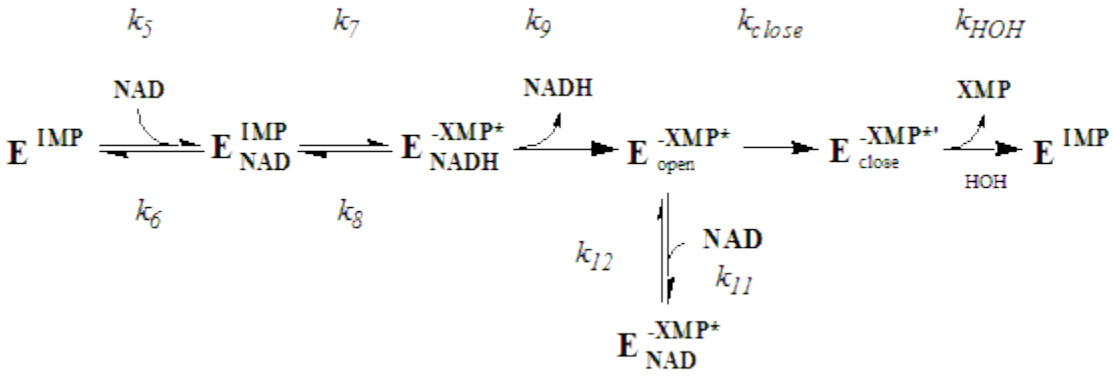

Scheme S2. Kinetic scheme used for global fits of the hIMPDH2 reaction by DynaFit.

REFERENCES

(1) Guillén Schlippe, Y. V., Riera, T. V., Seyedsayamdost, M. R., and Hedstrom, L. (2004) Substitution of the Conserved Arg-Tyr Dyad Selectively Disrupts the Hydrolysis Phase of the IMP Dehydrogenase Reaction. *Biochemistry 43*, 4511-21.

(2) Kuzmic, P. (1996) Program DYNAFIT for the analysis of enzyme kinetic data: application to HIV proteinase. *Anal Biochem 237*, 260-73.

(3) Umejiego, N. N., Li, C., Riera, T., Hedstrom, L., and Striepen, B. (2004) Cryptosporidium parvum IMP dehydrogenase: identification of functional, structural, and dynamic properties that can be exploited for drug design. *J Biol Chem 279*, 40320-7.

(4) King, and Altman. (1956) *J. Phys. Chem. 60*, 1375.

(5) Wang, W., and Hedstrom, L. (1997) Kinetic mechanism of human inosine 5'-monophosphate dehydrogenase type II: random addition of substrates and ordered release of products. *Biochemistry 36*, 8479-83.

(6) Hedstrom, L. (2002) Serine protease mechanism and specificity. *Chem Rev 102*, 4501-24.

(7) Northrop, D. B. (1975) Steady-state analysis of kinetic isotope effects in enzymic reactions. *Biochemistry 14*, 2644-51.

(8) Xiang, B., and Markham, G. D. (1997) Probing the mechanism of inosine monophosphate dehydrogenase with kinetic isotope effects and NMR determination of the hydride transfer stereospecificity. *Arch Biochem Biophys 348*, 378-82.